



Direct, Uncorrected, Molecule-Free Analysis of ^{236}U from Uranium-Bearing Particles with NAUTILUS: A New Kind of Mass Spectrometer

Journal:	<i>Analyst</i>
Manuscript ID	AN-ART-07-2018-001451.R1
Article Type:	Paper
Date Submitted by the Author:	31-Aug-2018
Complete List of Authors:	Willingham, David; U.S. Naval Research Laboratory, Materials Science and Technology Groopman, Evan; U.S. Naval Research Laboratory, Materials Science and Technology Grabowski, Kenneth; U.S. Naval Research Laboratory, Materials Science and Technology Sangély, Laure; International Atomic Energy Agency, Department of Safeguards

Direct, Uncorrected, Molecule-Free Analysis of ^{236}U from Uranium-Bearing Particles with NAUTILUS: A New Kind of Mass Spectrometer

D. Willingham¹, E.E. Groopman¹, K.S. Grabowski¹, L. Sangely²

¹U.S. Naval Research Laboratory, ²International Atomic Energy Agency

Abstract

We demonstrate use of the Naval Ultra-Trace Isotope Laboratory's Universal Spectrometer (NAUTILUS) at the U.S. Naval Research Laboratory (NRL) to measure ^{236}U directly from uranium-bearing particles free from molecular isobaric interferences. Particles with ^{235}U enrichments in the range of 0.32% to 3.28% and ^{236}U enrichments from no enrichment to 0.015% provided by the International Atomic Energy Agency (IAEA) were analyzed directly using the NAUTILUS. We report the experimental data here without correcting for molecular hydrides and/or applying any other background subtractions. The results from all samples agreed with the certified values within standard error save for the ^{236}U composition of the IRMM 023, which suffered from a combination of insufficient particle sizes and sub- $\mu\text{mol/mol}$ ^{236}U concentrations. We were able, however, to directly measure as low as three $\mu\text{mol/mol}$ of ^{236}U in individual particles regardless of the ^{235}U concentration. Our results are comparable with Large Geometry Secondary Ion Mass Spectrometry (LG-SIMS) and serve as baseline for a more comprehensive comparison between LG-SIMS and the NAUTILUS in the future. Moreover, we demonstrate the ability of the NAUTILUS to generate raster ion images with the same ease as traditional LG-SIMS instruments. By combining our ability to measure ^{236}U directly with raster ion imaging, we were able to detect a low intensity, small uranium-bearing particle in the presence of high molecular backgrounds for a non-ideal sample. This discovery could lead to more targeted and, therefore, less time intensive particle screening methodologies.

Keywords: NAUTILUS; nuclear Safeguards; Secondary Ion Mass Spectrometry (SIMS); Single-Stage Accelerator Mass Spectrometry (SSAMS); hydride correction; ion imaging

Introduction

Uranium-bearing particle analysis for international Safeguards traditionally employs a two-pronged approach. The first being Fission Track – Thermal Ionization Mass Spectrometry (FT-TIMS),¹ which excels in its ability to measure high precision uranium isotope ratios free from molecular isobaric interferences, but which suffers from extensive sample preparation requirements and relatively low throughput. The other being Large Geometry – Secondary Ion Mass Spectrometry (LG-SIMS),² which excels in its ability to measure uranium isotope ratios with much higher throughput and much less stringent sample preparation requirements than FT-TIMS, but which suffers from a number of molecular isobaric interferences that conspire to limit its overall precision and accuracy. The work presented herein is primarily concerned with improving high throughput uranium-bearing particle analysis (i.e. >5,000 particles per sample) and, therefore will draw a comparison only to standard LG-SIMS analysis. However, it is

1
2
3 44 important to note that FT-TIMS is a viable alternative to LG-SIMS when high precision is of
4 45 greater value than high throughput.
5
6

7 47 The application of LG-SIMS to the international Safeguards community requires an ability to
8 48 effectively screen for and detect uranium-bearing particles collected from Safeguards
9 49 inspections.³⁻¹⁰ A typical application of SIMS for nuclear Safeguards is to collect dust samples
10 50 taken using cotton swipes at enrichment facilities and analyze them to ensure that the level of
11 51 uranium enrichment remains within declared values. SIMS offers timely analyses of a
12 52 statistically significant number of uranium-bearing particles, the ability to distinguish between
13 53 uranium-bearing particles enriched or depleted in ²³⁵U, and high selectivity for particles of
14 54 interest within a vast background of environmental particles containing only natural uranium.
15 55 Despite advancements in automation of the SIMS screening process, long analysis times are
16 56 common and a single 1-inch round SIMS planchette can take upwards of 8-10 hours to fully
17 57 screen. Factors that contribute to these long analysis times include the fact that uranium-
18 58 bearing particles are measured one field-of-view (FoV) at a time and that there may be
19 59 hundreds to thousands of FoVs per planchette, and that ²³⁴U and ²³⁶U are typically present in
20 60 $\mu\text{mol/mol}$ concentrations and require long counting times. In addition, particles of interest
21 61 identified in the screening process require re-analysis in microprobe mode, which involves a set
22 62 of different instrument analytical parameters.¹¹⁻¹³
23
24
25
26
27

28 64 The most pressing challenge for SIMS, however, is that the ²³⁵U¹H molecule complicates the
29 65 measurement of ²³⁶U. The presence of ²³⁶U is characteristic of uranium reprocessed from spent
30 66 nuclear fuel and is, therefore, of interest with respect to environmental sampling.^{14, 15} High-
31 67 resolution mass spectrometry techniques traditionally approach the challenge of molecular
32 68 isobaric interferences by striving to increase the mass resolving power of the analysis. For
33 69 example, ²⁰⁸Pb²⁸Si, ²⁰⁴Pb¹⁶O₂, ²³⁵U¹H and ²³⁶U all of the same nominal mass at 236, but have
34 70 different exact masses at 235.953, 235.963, 236.026 and 236.052 respectively. For instance, at
35 71 a resolving power of 500, these masses are all overlapped and cannot be distinguished from
36 72 one another. Increasing the resolving power to 3000 separates out ²⁰⁸Pb²⁸Si and ²⁰⁴Pb¹⁶O₂
37 73 leaving ²³⁵U¹H and ²³⁶U overlapping. It is much more difficult to separate out the hydride
38 74 molecule from its adjacent isotope. In fact, it would take a resolving power of greater than
39 75 38,000 to distinguish between ²³⁵U¹H and ²³⁶U. Unfortunately, as the resolving power increases,
40 76 the ion transmission decreases. Even under ideal conditions, the ion transmission of a CAMECA
41 77 ims-1280 is essentially zero at the mass resolution required to separate ²³⁵U¹H from ²³⁶U.¹⁶
42
43
44
45

46 79 The NAUTILUS at NRL represents an alternative methodology for removing molecular isobaric
47 80 interferences.¹⁷ The NAUTILUS is a combination of a small geometry SIMS analyzer and a Single
48 81 Stage Accelerator Mass Spectrometry (SSAMS) detector. It works in much the same way as a
49 82 traditional SIMS instrument. Primary ions sputter secondary ions into the mass spectrometer
50 83 where they are energy and mass filtered. However, in the place where detection occurs by an
51 84 electron multiplier (EM) or faraday cup (FC), the secondary ions pass into the SSAMS. The
52 85 secondary ions exiting the SIMS accelerate by 300 keV and then enter the gas stripper tube.
53 86 Here molecular dissociation with minimal scattering loss occurs as the higher energy secondary
54 87 ions interact with gas (i.e. Ar) in the stripper tube. The amount of molecular dissociation is
55
56
57
58
59
60

1
2
3 88 exponentially proportional to gas flow in the stripper tube and is much higher than ion
4 89 transmission loss though the rest of the SSAMS instrument. Previous work has shown that a 10^5
5 90 reduction in molecular ion signal is achievable with only 0.2 sccm (7.03×10^{15} atoms/cm²) of Ar
6 91 gas flow in the stripper tube, while only reducing transmission of atomic species by
7 92 approximately 60 percent.^{18, 19} In this way, the NAUTILUS nearly eliminates the contribution of
8 93 ²³⁵U¹H to the mass-to-charge (m/z) 236 mass channel and results in molecule-free analysis of
9 94 uranium-bearing particles at a resolving power of only 500.
10
11
12 95

13 96 Although microprobe mode, which is a non-imaging mode, is usually required to determine the
14 97 uranium isotopes present in any given particle, raster ion imaging is critical to perform the
15 98 initial automated screening of the particle population.^{4, 6, 7, 20} Therefore, it is important to
16 99 implement raster ion imaging on the NAUTILUS this is comparable, at minimum, to what is
17
18 100 available by traditional SIMS instrumentation. Because the front end of the NAUTILUS is a SIMS
19 101 instrument, the mechanics of generating a raster ion image are identical. The primary ion beam
20 102 follows a software determined raster pattern by applying voltage to the primary ion raster
21 103 plates. Voltages applied to the secondary dynamic transfer plates compensate for variations in
22 104 the location of the primary ions during the raster in order to maintain a consistent extraction of
23 105 the secondary ions into the mass spectrometer. At this point, detection of the secondary ions
24 106 either occurs at the EM at the end of the SIMS instrument or at the EM at the end of the SSAMS
25 107 instrument. Synchronization of the primary ion raster pattern and the pulse train on the
26 108 detection EM allows for the reconstruction of the raster ion image as ion intensity as a function
27 109 of x and y image pixel position. Not only can we image at two separate locations (SIMS-EM and
28 110 SSAMS-EM), we can electrostatically switch between the two, effectively producing On/Off
29 111 raster ion images where the SIMS image is characteristic of a convolution of atoms and
30 112 molecules and the SSAMS image is a truly molecule-free isotope image.
31
32
33
34 113

35 114 **Experimental**

36 115
37 116 The NAUTILUS combines a modified CAMECA ims-4f SIMS and a ± 300 keV National
38 117 Electrostatics Corporation (NEC) SSAMS with the ability to analyze singly charged ions up to
39 118 mass 300. Unlike traditional tandem AMS relegated to measuring only negative ions, the SSAMS
40 119 can accept either positive or negative ions from the SIMS. This is beneficial to SIMS as the
41 120 majority of secondary ions observed for actinides are single-charge, positive ions. A complete
42 121 description of the NAUTILUS has been previous reported.^{18, 19, 21} Briefly, the secondary ions
43 122 leave the sample at 4.5 keV of energy and are subsequently filtered by their energy and mass in
44 123 the SIMS and then electrostatically deflected onto one of a suite of detectors including an EM, a
45 124 FC, or a microchannel plate (MCP) beam imager. Alternatively, the ions deflect into the SSAMS
46 125 after leaving the SIMS instrument. Here the secondary ions accelerate by 300 kV via 44
47 126 electrodes on a resistor chain from a high-voltage bias on the deck to Earth/SIMS ground. The
48 127 accelerated secondary ions then focus into the center of a gas-stripping cell consisting of a
49 128 number of concentric, differentially pumped cylinders, filled with Ar gas. The NAUTILUS then
50 129 filters atomic ions by their mass and energy and analyzes them at the end of the SSAMS by
51 130 either an EM or a MCP beam imager.
52
53
54
55 131
56
57
58
59
60

1
2
3 132 The International Atomic Energy Agency (IAEA) provided NRL with a number of uranium-
4 133 bearing particle samples for evaluation and comparison to their CAMECA ims-1280 SIMS
5 134 instrument. The samples originate from various chemical forms ranging from uranium oxide
6 135 (U_3O_8), uranium hexafluoride (UF_6) and a uranium nitrate solution. It should be mentioned,
7 136 however, that the UF_6 (IRMM CRM-023) standard was dissolved in a nitrate solution and then
8 137 converted into uranium oxides in the process of producing particles. Furthermore, the uranium
9 138 nitrate solution (IRMM CRM-183) standard underwent a similar conversion to uranium oxide
10 139 particles prior to analysis. The U_3O_8 particle preparation consisted of a simple vacuum
11 140 impaction of the solid particles onto a 1-inch diameter vitreous carbon planchette. The nitrate
12 141 solutions were converted into monodispersed particles at the Forschungszentrum Juelich
13 142 (Germany) using a vibration orifice aerosol generator (VOAG) passing through a drying column.
14 143 The particle preparation then proceeded by vacuum impaction in a similar fashion as the other
15 144 uranium-bearing samples. Additionally, the IAEA shared glass particle samples provided to them
16 145 by The National Institute for Standards and Technology (NIST). The NIST sample preparation
17 146 method involved directly depositing the glass powder with a swab by gently sprinkling the
18 147 target surface. The U_3O_8 content in the glass is 10 wt. % with a remaining composition of 20 wt.
19 148 % lithium dioxide (LiO_2), 16.5 wt. % boric oxide (B_2O_3), 3.5 wt. % aluminum oxide (Al_2O_3), 49.0
20 149 wt. % silicon dioxide (SiO_2) and 1 wt. % XO (where X is either barium, calcium or magnesium
21 150 depending on the specific sample number). The isotopic composition of the NIST glass samples
22 151 is known to be "near natural" with the ^{236}U composition of NIST-4 and NIST-5 known to be 5.6
23 152 ppm and 2.8 ppm respectively. The particles range in ^{235}U enrichment from 0.32% to 3.28% and
24 153 in ^{236}U enrichment from no enrichment to 0.015%. Table-1 contains the full list of particle
25 154 standards acquired from the IAEA. We estimate that the particles ranged in size from 0.8 – 5-
26 155 μm in diameter, but have not confirmed this using Scanning Electron Microscopy (SEM). If this
27 156 size range is correct, we expect $\sim 6 \times 10^7$ to 4×10^8 secondary uranium ions per particle assuming a
28 157 1% uranium ionization efficiency.⁵ In practice, these numbers will be even lower due to isotopic
29 158 variations and duty cycle considerations; however, it was common for us to observed count
30 159 rates $>10,000$ counts per second for ^{238}U from an individual particle. NRL received the prepared
31 160 planchettes shipped directly from the IAEA and analyzed them on the NAUTILUS without
32 161 further manipulation.

33 162
34 163 NRL analyzed all particles using an identical procedure. We used NIST CRM 850 to calibrate the
35 164 uranium isotope masses at ^{234}U , ^{235}U , ^{236}U , ^{238}U and $^{238}U^1H$ for both the SIMS and SSAMS
36 165 sections of NAUTILUS. We used the optical microscope on the SIMS to locate individual
37 166 particles for analysis coarsely and used the real-time MCP beam image for fine adjustment of
38 167 the particle location. Analyses of individual particles used a 10 x 10- μm raster of a 1-nA, 10 keV
39 168 O^- primary ion beam. Save for the use of O^- in place of O_2^+ , this procedure is identical to that
40 169 used by the SIMS analysis team at the IAEA. The analysis of particles continued until we
41 170 counted a statistically relevant number of ions for each isotope or consumed the particle
42 171 completely.

43 172
44 173 Additional SIMS parameters used for these measurements are as follows. On the primary side
45 174 we used mass aperture one (750 μm) and primary aperture two (200 μm). On the secondary
46 175 side we used field aperture one (1800 μm), contrast aperture one (400 μm), energy slit of ~ 100

176 eV, entrance slit of ~350 μm , exit slit of ~700 μm for a 2:1 ratio with the entrance slit and an
 177 imaged field of 75 μm . Since we are using dynamic transfer, no clipping of the secondary ion
 178 beam occurs even for the 250- μm raster for imaging, since the 75 μm -imaged field is larger
 179 than the primary beam size. The mass resolving power with these conditions is ~500. Without
 180 aberrations, the transmittance would be ~87.5%.

181
 182 In order to demonstrate the utility of raster ion imaging on the NAUTILUS, we produced a
 183 particle dispersion on a single vitreous carbon planchette consisting of NIST CRM U500 particles
 184 along with crushed monazite particles. The monazite particles represent a source of natural
 185 uranium with no ^{236}U , but with a variety of other elements (i.e. rare earth elements and
 186 actinides). Previous analysis of this monazite (Smithsonian National Museum of Natural History,
 187 NMNH #R14013) by SIMS reveals a peak at nearly every mass making it challenging to measure
 188 uranium isotopes.¹⁹ Production of the single planchette started with U500 particles drop dried
 189 from a liquid suspension and followed by a similar suspension containing crushed monazite
 190 powder in place of the U500 particles. Raster ion imaging of these overlapping particle
 191 populations occurred by using a 1-nA, 10 keV O^- primary ion beam, similar to the parameters
 192 for single particle analysis. Collected images used a raster pattern of 256 x 256 pixels over an
 193 area of 250 x 250 μm . We selected the isotopes ^{232}Th , ^{235}U , ^{236}U and ^{238}U for comparison
 194 between SIMS and NAUTILUS raster ion imaging. Interleaving these images electrostatically
 195 allowed for direct comparison within each run reducing the risk of biasing the image analysis
 196 toward any single outcome.

NIST certified values for U030a and U010

CRM	$^{235}\text{U}/^{238}\text{U}$	^{234}U %	^{235}U %	^{236}U %	^{238}U %
U010	0.010140	0.00541	1.0037	0.00681	98.984
U030a	0.031367	0.02778	3.0404	0.000599	96.9312

IRMM certified values for 023 and 183

IRMM	$^{235}\text{U}/^{238}\text{U}$	^{234}U %	^{235}U %	^{236}U %	^{238}U %
023	0.0338881	0.032827	3.2760	0.00001115	96.6911
183	0.0032157	0.0019688	0.32049	0.0147858	99.66276

Other uranium containing particles for QA/QC

	$^{235}\text{U}/^{238}\text{U}$	^{234}U %	^{235}U %	^{236}U %	^{238}U %
NIST-4	0.007436	0.00551	0.7381	0.00056	99.2559
NIST-5	0.007347	0.00543	0.7293	0.00028	99.2650
YC9081	0.007161	0.0055	0.711	N/A	99.284

Table-1: The certified values (where applicable) for the NIST CRM, IRMM and other uranium containing QA/QC standards used by the IAEA.

197 Results and discussion

198
 199 The particle samples acquired by NRL from the IAEA represent a variety of U-bearing standards
 200 for quality assurance (QA) and quality control (QC) purposes. The NIST CRM standards
 201 demonstrate a measurement capability over a range of ^{235}U enrichments (that overlaps with
 202 those typically encountered by IAEA inspectors). The IRMM standards, although analyzed in
 203 their final oxidized form, represent an ability to analyze particles derived from alternative
 204 sources of uranium. We used the NIST-4 and NIST-5 glass particles to evaluate our ability to
 205 detect ppm levels of ^{236}U . For all of these samples, we postulate the same core question: Can
 206 the NAUTILUS efficiently dissociate the $^{235}\text{U}^1\text{H}$ interference on ^{236}U for samples of interest to
 207 the international Safeguards community?
 208

209 Figure-1 shows the cumulative data for all of the runs (3-4 particles per sample) of all of the
 210 following samples (yellowcake [YC], CRM U010, CRM 030a, IRMM 183 and IRMM 023). The
 211 plots show the uranium isotope ratios of $^{234}\text{U}/^{238}\text{U}$ vs. $^{235}\text{U}/^{238}\text{U}$ in Figure-1a and $^{236}\text{U}/^{238}\text{U}$ vs.
 212 $^{235}\text{U}/^{238}\text{U}$ in Figure-1b. Dashed lines indicate the locations of the certified reference values
 213 where applicable. The IRMM 023 certified reference value for ^{236}U of approximately 100
 214 nmol/mol is located essentially at the zero mark in Figure-1b. Error bars represent the standard
 215 error for each individual particle measurement (many of the error bars are within the graph
 216 symbols and are not visible). These errors result primarily from counting statistics and scale
 217 with the square root of the number of counts obtained for each particle analysis. We can see
 218 that all of the measured values agree well with the certified values within error save for the
 219 IRMM 023, which has a bit more scatter than the other sample materials. A lack of ion counts
 220 drives the uncertainty in these measurements. The IRMM 023 particles proved relatively small
 221 compared to the other samples and an individual particle is often completely exhausted before

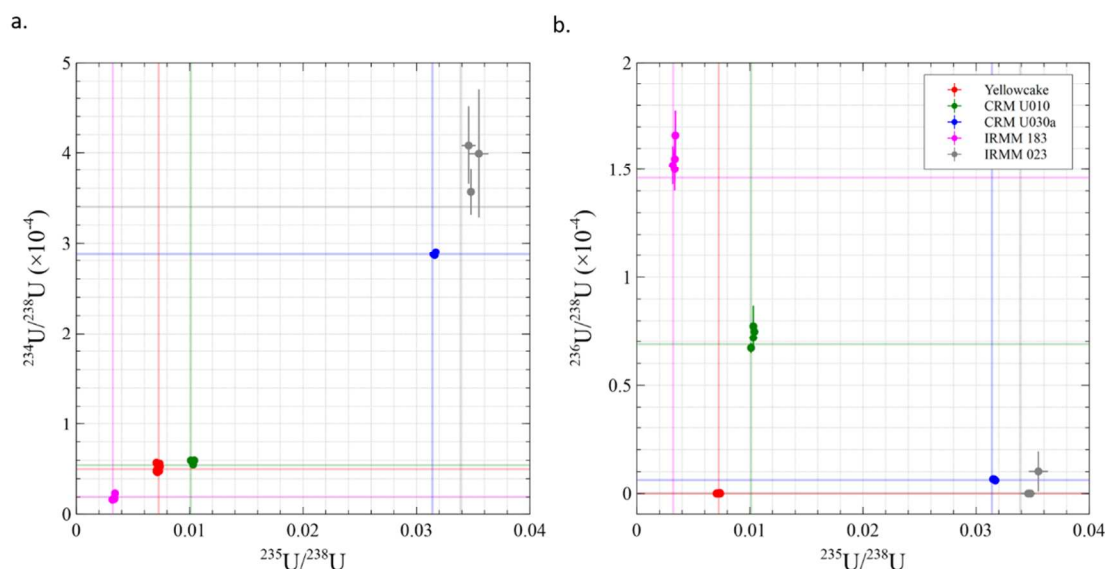


Figure-1: Plots show the uranium isotope ratios of $^{234}\text{U}/^{238}\text{U}$ (a) and $^{236}\text{U}/^{238}\text{U}$ (b) vs. $^{235}\text{U}/^{238}\text{U}$ for QA/QC samples. The dashed lines indicate the location of the certified reference values.

222 obtaining an adequate number of ion counts for a high precision measurement.

223
224 It is important to mention, that the ^{236}U values reported for these samples remain uncorrected.
225 This is in contrast to traditional LG-SIMS measurements that require a hydride correction that
226 relies on an accurate measurement of the ^{235}U , ^{236}U , ^{238}U and $^{238}\text{U}^1\text{H}$ signals. Although
227 previously demonstrated to be effective over a wide range of ^{235}U enrichments, the hydride
228 correction is limited in cases where the ^{236}U signal is present at trace levels and the ^{235}U
229 enrichment is relatively high. Particles containing less than approximately one $\mu\text{mol/mol}$ of ^{236}U
230 could not be corrected using traditional methods.⁵ Additionally, the hydride correction would
231 not be effective for samples containing both ^{238}U and ^{239}Pu , as the nominal mass channel at m/z
232 236 would contain $^{235}\text{U}^1\text{H}$ and ^{236}U and the nominal mass channel at m/z 239 would contain
233 $^{238}\text{U}^1\text{H}$ and ^{239}Pu .²² We contest that for specific cases; only a direct ^{236}U measurement using the
234 NAUTILUS would provide adequate results.

235
236 Figure-2 shows the cumulative data for all of the runs (3-7 particles per samples) of all the
237 following samples (YC, NIST-5, NIST-6 and CRM U030a). The plots show the uranium isotope
238 ratios of $^{236}\text{U}/^{238}\text{U}$ vs. $^{235}\text{U}/^{238}\text{U}$. Figure-2a compares the first three samples (YC, NIST-5 and
239 NIST-6) and indicates that the known values of three $\mu\text{mol/mol}$ and six $\mu\text{mol/mol}$ for NIST-6 and
240 NIST-5 respectively agreed with the NAUTILUS results. As a reference, we included the YC
241 particle data to show our uncorrected, ^{236}U background. Our count rate for m/z 236 was
242 essentially zero over the course of measuring samples with no ^{236}U . Figure-2b compares all of
243 the data in Figure-2a, but adds in the data for the CRM U030a particles. Here, a direct
244 comparison between CRM U030a and NIST-5 can be made where each contains approximately
245 six $\mu\text{mol/mol}$ of ^{236}U , but where the CRM U030a contains approximately four times the amount
246 of ^{235}U than the NIST-5 particles. Direct ^{236}U measurement using NAUTILUS are unaffected by
247 the amount of ^{235}U over a dynamic range of approximately 10^5 . This means that if we assume a
248 hydride contribution of approximately 1:1000 $^{235}\text{U}^1\text{H}$ counts relative to ^{235}U , a direct ^{236}U
249 measurement at six $\mu\text{mol/mole}$ would be possible even for highly enriched uranium-bearing
250 particles. Arguably, a more interesting contention is that given enough atoms, a direct, sub-100
251 nmol/mol ^{236}U measurement on a 3% ^{235}U enriched particle is possible. We intend to test this
252 hypothesis in the future by obtaining larger IRMM 023 particles with a certified ^{236}U
253 composition of 111.5 nmol/mol and a ^{235}U composition of 3.28 %. A number of other studies
254 have focused on particle analysis of relatively pure materials under ideal conditions (i.e. U_3O_8
255 particle vacuum impaction onto vitreous carbon planchettes). However, our interests extend to
256 systems that are more complicated. To that end, Figure-3 shows several images of CRM U500
257 particles dispersed on a background of monazite particles. We focused on four main isotopes to
258 image (^{232}Th , ^{235}U , ^{236}U and ^{238}U); however, as mentioned above, analysis of the monazite bulk
259 material has revealed that there is a peak at nearly every mass. Each pane of Figure-3 compares
260 the SIMS image taken prior to molecular dissociation and the molecule-free SSAMS image taken

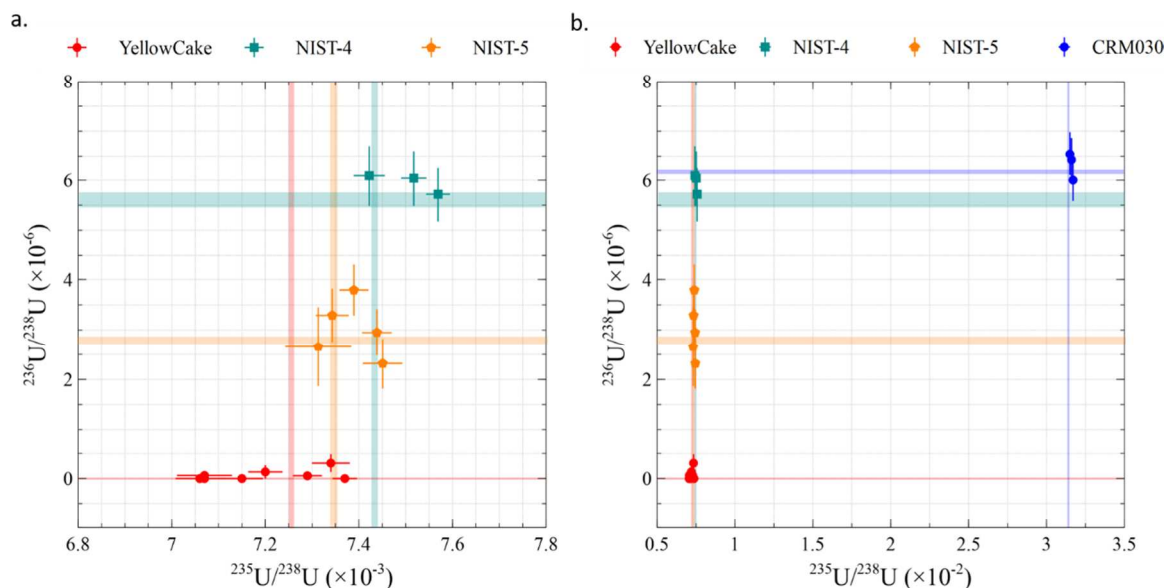


Figure-2: Plots show the uranium isotope ratios of $^{236}\text{U}/^{238}\text{U}$ vs. $^{235}\text{U}/^{238}\text{U}$ for YC, NIST-5 and NIST-6 (a) and for an additional sample CRM U030a (b). The dashed lines indicate the location of the known values for the ^{236}U concentrations.

at the end station of the NAUTILUS. Overall, the ^{232}Th , ^{235}U and ^{238}U images in Figure-3a, b and d, respectively, look comparable, save for a greatly reduced background for the SSAMS images compared to the SIMS ones. This is, primarily, because most of the CRM U500 particles are large and have high intensities. This makes them easily distinguished from the background, at least visually. The one exception to this observation is the ^{236}U signals shown in Figure-3c. Arrows point to three particles of interest in this pair of images. Although only represented by a handful of pixels, the SSAMS image differentiates the three distinct particles, whereby the SIMS image is only capable of identifying two particles. The SIMS image backgrounds for the m/z of 236 are simply too high for the lowest intensity particle.

Taking a closer look, Figure-4 zooms in on the three particles of interest. Analysis of this region commenced by alternating SIMS m/z 236 measurements in Figure-4b and d with SSAMS m/z 236 measurements in Figure-4a and c. We split these analyses into the first three iterations in Figure-4a and b and the last three iterations in Figure-4c and d and discovered that we completely consumed the small, less intense CRM U500 particle in the process. This observation is present in the SSAMS images comparing Figure-4a and c where there are originally three distinct particles, but only two remain after a few image cycles. This finding is in contrast to the SIMS images comparing Figure-4b and d where there are only two observable particles in either image. A closer examination of a sub-region of the images indicated by the dashed box in Figure-4d (we interrogated the region for each image, although have only shown it in a single image for demonstration purposes) reveals the reason for the discrepancy

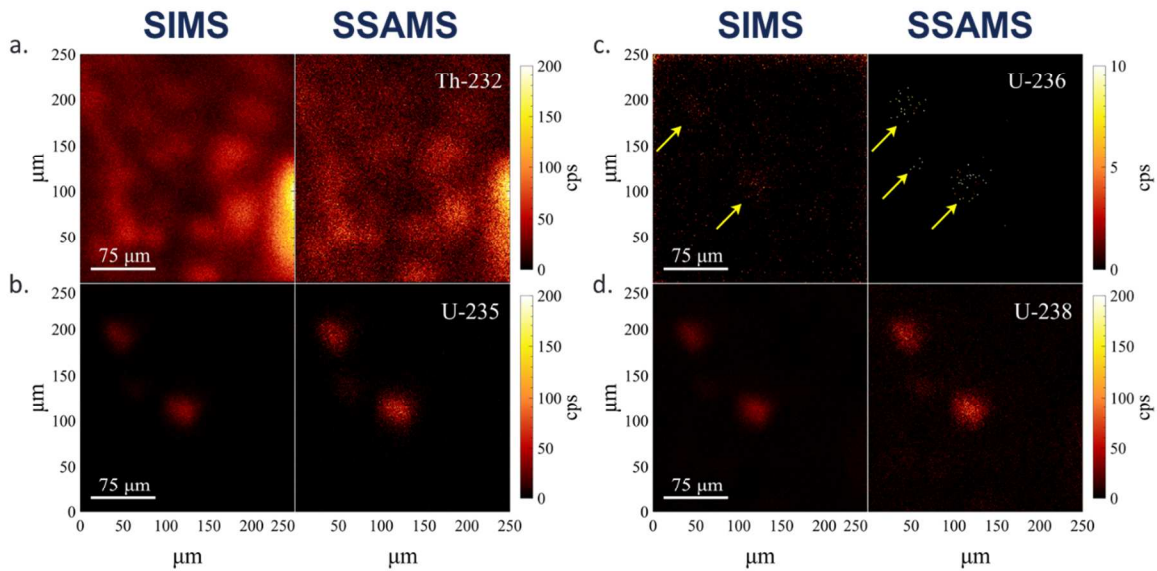


Figure-3: Plots show the comparison between SIMS and SSAMS images for ^{232}Th , ^{235}U , ^{236}U and ^{238}U for a, b, c and d respectively. The sample is NIST CRM U500 particles in the presence of monazite particles. The yellow arrows indicate particle identified by m/z 236.

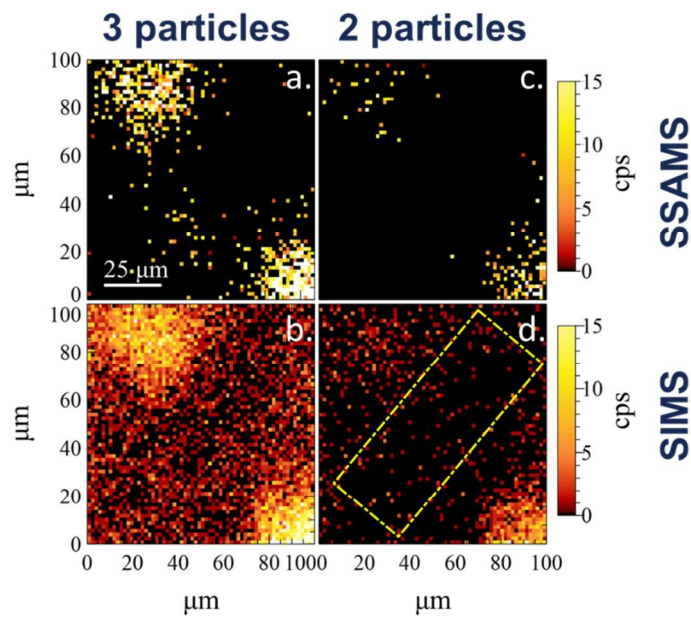


Figure-4: Plots show the comparison between SIMS (b, d) and SSAMS (a, c) images for ^{236}U for the first three (a, b) and last three (c, d) image iterations. The dashed yellow box shows the region of interest for the two-dimension data present in Figure-5.

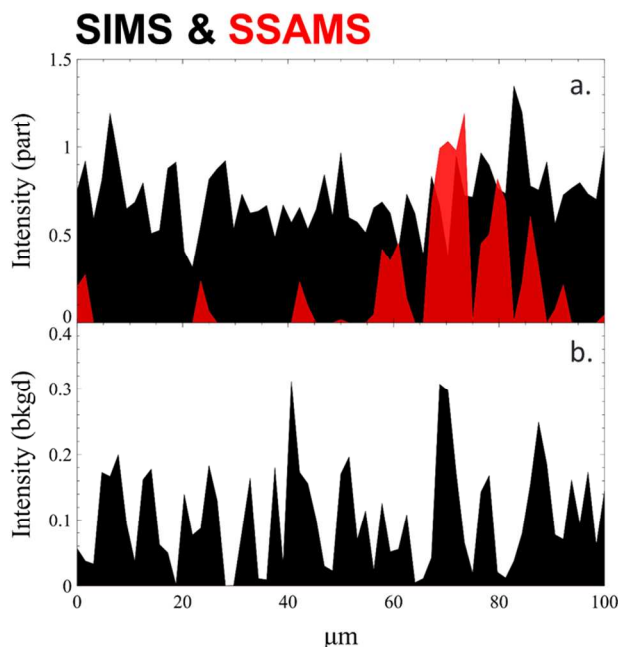


Figure-5: Plots show the line scan comparison between SIMS (black) and SSAMS (red) from Figure-4 first three (a) and last three (b) image iterations. There is no SSAMS signal in the last three (b).

282 between the SIMS and SSAMS images. Figure-5 shows the comparison of these sub-regions
 283 SIMS vs. SSAMS for the first three image cycles in Figure-5a and for the last three image cycles
 284 in Figure-5b. The two-dimensional data in Figure-5 represents the sum of all of the counts along
 285 the y-axis of the sub-region rectangle plotted versus the x-axis position in order to form a thick
 286 line scan of the area between the two more intense CRM U500 particles. As previously
 287 mentioned, the SSAMS backgrounds are essentially zero for the mass channel at m/z 236
 288 allowing for the detection of the low intensity CRM U500 particle. SIMS, on the other hand has
 289 higher backgrounds that, in this case, obscure the low intensity particle allowing for the
 290 detection of only two particles. While we are aware that these data represent only one
 291 unidentified particle in one FoV, extrapolation of these data to the total scan area of a single
 292 vitreous carbon planchette with well over a thousand such FoVs could conservatively result in
 293 at least tens of unidentified particles. Additionally, the unidentified particles would be
 294 disproportionately less intense and, therefore, smaller than the average population of
 295 identified particles introducing a significant size selection bias into the SIMS only data.

296 297 Conclusions

298
 299 We have demonstrated the utility of the NAUTILUS for the direct, uncorrected measurement of
 300 ^{236}U in concentrations as low as a three $\mu\text{mol/mol}$ from IAEA QA/QC standards ranging in ^{235}U
 301 enrichment from 0.32% to 3.28%. We have shown that single particle analysis by NAUTILUS is
 302 no more complicated and only slightly more time consuming (primarily due to mono-collection
 303 vs. multi-collection detector variations) than traditional LG-SIMS analysis and, therefore, is
 304 compatible with the already existing IAEA particle analysis protocols. Our ability to directly

1
2
3 305 measure ^{236}U is unaffected by the amount of ^{235}U present in the sample. Moreover, where the
4 306 LG-SIMS community has largely focused in the literature on investigating the hydride correction
5 307 in the ideal case (pure oxide samples well separated on a clean substrate), we have considered
6 308 two more probing questions. What if the sample has multiple actinides (i.e. U and Pu) and/or
7 309 the sample matrix is complex with many more opportunities for interfering species? What if an
8 310 analysis calls for particle distributions not well separated from each other and not sufficiently
9 311 well removed from a more complex background material? Future analysis directly comparing
10 312 our results with those of LG-SIMS will be critical to answering these questions in a detailed and
11 313 comprehensive manner.
12
13 314

14 315 As required for automated screening of particle distributions by LG-SIMS, we have
15 316 demonstrated that the NAUTILUS is capable of raster ion imaging comparable to traditional LG-
16 317 SIMS methods. Direct analysis of the ^{236}U present in CRM U500 particles in a field of monazite
17 318 particles illustrates our ability to detect low intensity, small particles free from background
18 319 signals. This opens the door for advanced screening methodologies. For example, instead of
19 320 screening for ^{234}U , ^{235}U , ^{236}U , ^{238}U and $^{238}\text{U}^1\text{H}$ as is typical for LG-SIMS analyses, one could
20 321 simply screen for ^{236}U with the NAUTILUS. This method would likely allow for the use of faster
21 322 scanning speeds, therefore, decreasing the total time to screen the total area of a vitreous
22 323 carbon planchette. Knowing that nearly every pixel is a positive particle identification, leads to a
23 324 much more targeted screening approach than is currently available by traditional LG-SIMS.
24 325 Additionally, we have demonstrated the ability of the NAUTILUS to detect low intensity, small
25 326 particles that are within the background signal of comparable SIMS measurements. While we
26 327 are aware that LG-SIMS will not likely encounter this challenge for pure oxide particles on a
27 328 clean substrate, we contend that the capabilities of the NAUTILUS may supplant traditional LG-
28 329 SIMS when the need to analyze non-ideal samples arises.
29
30 330

31 331 For clarity, consider the following hypothetical scenario. There are two particle populations
32 332 with >10,000 particles each, they have been enriched to the same $^{235}\text{U}/^{238}\text{U}$ ratio and,
33 333 therefore, cannot be discriminated based on their major uranium isotope composition alone.
34 334 These particle populations differ in the fact that one population was enriched from fuel that
35 335 had not been reprocessed (i.e. no ^{236}U) and the other from fuel that had been processed (i.e.
36 336 containing ^{236}U). If we simply wanted to answer the question, "was this uranium-bearing
37 337 particle population derived from fuel that had been reprocessed," we could use the
38 338 aforementioned particle searching methodology for ^{236}U with the NAUTILUS to get a fast, yes or
39 339 no determination without the need to make high precision measurements of all of the uranium
40 340 isotopes. In this scenario, if we observe ^{236}U in the first, fast-pass scan, we then revisit the
41 341 individual particles for a more thorough high precision measurement. For this type of "real-
42 342 world" application, the NAUTILUS would be well suited to add value to the already formidable
43 343 combination of FT-TIMS and LG-SIMS.
44
45 344

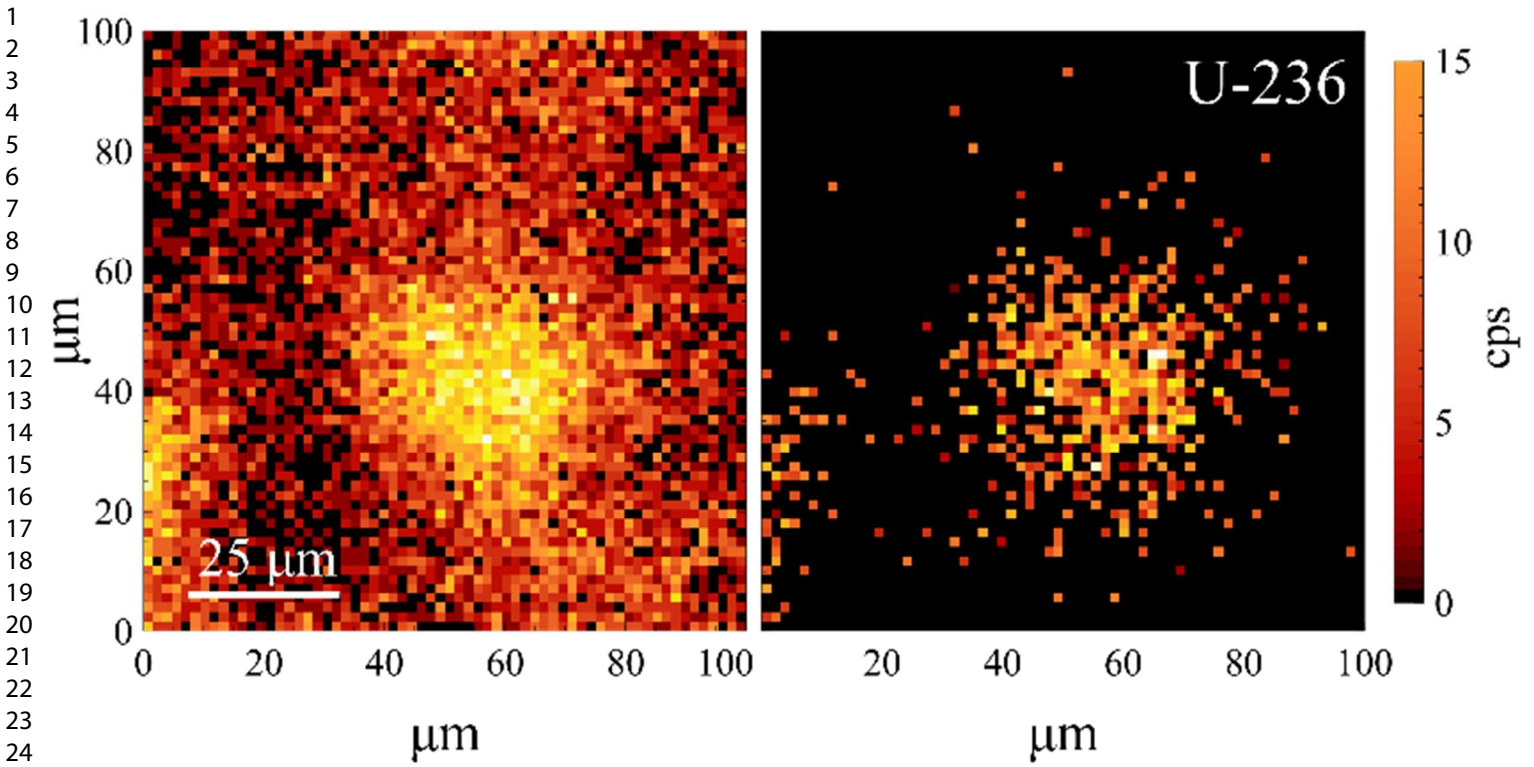
46 345 **Acknowledgements**

47 346
48 347 Base Programs Research and Development funding from the Office of Naval Research through
49 348 the U.S. Naval Research Laboratory supported this work. We would like to thank the
50
51
52
53
54
55
56
57
58
59
60

1
2
3 349 International Atomic Energy Agency and the National Institute of Standards and Technology for
4 350 providing actinide samples, and the Smithsonian National Museum of Natural History for
5
6 351 providing the monazite.
7

8 References

- 9
- 10 1. Y. Chen, Y. Shen, Z. Y. Chang, Y. G. Zhao, S. L. Guo, J. Y. Cui and Y. Liu, *Radiat Meas*, 2013, **50**, 43-45.
- 11
- 12 2. P. Peres, P. M. L. Hedberg, S. Walton, N. Montgomery, J. B. Cliff, F. Rabemananjara and M. Schuhmacher, *Surf Interface Anal*, 2013, **45**, 561-565.
- 13
- 14 3. P. M. L. Hedberg, P. Peres, F. Fernandes, N. Albert and C. Vincent, *J Vac Sci Technol B*, 2018, **36**.
- 15 4. J. G. Tarolli, B. E. Naes, L. Butler, K. Foster, C. M. Gumbs, A. L. Howard and D. Willingham, *Analyst*, 2017, **142**, 1499-1511.
- 16 5. D. S. Simons and J. D. Fassett, *J Anal Atom Spectrom*, 2017, **32**, 393-401.
- 17 6. D. Willingham, B. E. Naes, P. G. Heasler, M. M. Zimmer, C. A. Barrett and R. S. Addleman, *J Vac Sci Technol B*, 2016, **34**.
- 18 7. J. G. Tarolli, B. E. Naes, B. J. Garcia, A. E. Fischer and D. Willingham, *J Anal Atom Spectrom*, 2016, **31**, 1472-1479.
- 19 8. N. Sharp, J. D. Fassett and D. S. Simons, *J Vac Sci Technol B*, 2016, **34**.
- 20 9. P. M. L. Hedberg, P. Peres, F. Fernandes and L. Renaud, *J Anal Atom Spectrom*, 2015, **30**, 2516-2524.
- 21 10. F. Esaka and M. Magara, *Talanta*, 2014, **120**, 349-354.
- 22 11. Y. Ranebo, M. Eriksson, G. Tamborini, N. Niagolova, O. Bildstein and M. Betti, *Microscopy and Microanalysis*, 2007, **13**, 179-190.
- 23 12. M. Betti, A. D. Heras and G. Tamborini, *Appl Spectrosc Rev*, 2006, **41**, 491-514.
- 24 13. G. Tamborini, D. L. Donohue, F. G. Rudenauer and M. Betti, *J Anal Atom Spectrom*, 2004, **19**, 203-208.
- 25 14. M. A. C. Hotchkis, D. Child, D. Fink, G. E. Jacobsen, P. J. Lee, N. Mino, A. M. Smith and C. Tuniz, *Nucl Instrum Meth B*, 2000, **172**, 659-665.
- 26 15. P. Steier, M. Bichler, L. K. Fifield, R. Golser, W. Kutschera, A. Priller, F. Quinto, S. Richter, M. Srnckif, P. Terrasi, L. Wacker, A. Wallner, G. Wallner, K. M. Wilcken and E. M. Wild, *Nucl Instrum Meth B*, 2008, **266**, 2246-2250.
- 27 16. M. C. Liu, K. D. McKeegan, T. M. Harrison, G. Jarzebinski and L. Vltava, *Int J Mass Spectrom*, 2018, **424**, 1-9.
- 28 17. E. E. Groopman, D. G. Willingham, A. P. Meshik and O. V. Pravdivtseva, *Proc Natl Acad Sci U S A*, 2018, **115**, 8676-8681.
- 29 18. A. J. Fahey, E. E. Groopman, K. S. Grabowski and K. C. Fazel, *Anal Chem*, 2016, **88**, 7145-7153.
- 30 19. E. E. Groopman, K. S. Grabowski, A. J. Fahey and L. Koop, *J Anal Atom Spectrom*, 2017, **32**, 2153-2163.
- 31 20. D. G. Willingham, Naes, Benjamin E., Tarolli, Jay G., *Proceedings of the 57th Annual Meeting of the Institute of Nuclear Materials Management*, 2016, **1**, 1971-1983.
- 32 21. K. S. Grabowski, E. E. Groopman and A. J. Fahey, *Nucl Instrum Meth B*, 2018, **414**, 155-160.
- 33 22. Y. Ranebo, N. Niagolova, N. Erdmann, M. Eriksson, G. Tamborini and M. Betti, *Anal Chem*, 2010, **82**, 4055-4062.
- 34
- 35
- 36
- 37
- 38
- 39
- 40
- 41
- 42
- 43
- 44
- 45
- 46
- 47
- 48
- 49
- 50
- 51
- 52
- 53
- 54
- 55
- 56
- 57
- 58
- 59
- 60



The Naval Ultra-Trace Isotope Laboratory's Universal Spectrometer (NAUTILUS) can measure ^{236}U directly from uranium-bearing particles free from molecular isobaric interferences.

1
2
3
4
5
6
7
8
9
10
11
12
13
14
15
16
17
18
19
20
21
22
23
24
25
26
27
28
29
30
31
32
33
34
35
36
37
38
39
40
41
42
43
44
45
46
47
48
49
50
51
52
53
54
55
56
57
58
59
60